REPORT DOCUMENTATION PAGE

Form Approved OMB NO. 0704-0188

1. REPORT DATE (DD-MM-YYYY)	2. REPORT TYPE	3. DATES COVERED (From - To)
17-11-2021	Final Report	20-Jul-2017 - 19-Jul-2021

4. TITLE AND SUBTITLE
Final Report: Self-Assembly of Colloidal Diamond and Related Lattices for 3-D Photonic Band Gap Materials

5a. CONTRACT NUMBER
W911NF-17-1-0328

5b. GRANT NUMBER

5c. PROGRAM ELEMENT NUMBER
611102

6. AUTHORS

5d. PROJECT NUMBER

5e. TASK NUMBER

5f. WORK UNIT NUMBER

7. PERFORMING ORGANIZATION NAMES AND ADDRESSES
New York University
665 Broadway
Suite 801
New York, NY 10012 -2331

8. PERFORMING ORGANIZATION REPORT NUMBER

9. SPONSORING/MONITORING AGENCY NAME(S) AND ADDRESS (ES)
U.S. Army Research Office
P.O. Box 12211
Research Triangle Park, NC 27709-2211

10. SPONSOR/MONITOR'S ACRONYM(S)
ARO

11. SPONSOR/MONITOR'S REPORT NUMBER(S)
70394-MS.3

12. DISTRIBUTION AVAILIBILITY STATEMENT
Approved for public release; distribution is unlimited.

13. SUPPLEMENTARY NOTES
The views, opinions and/or findings contained in this report are those of the author(s) and should not contrued as an official Department of the Army position, policy or decision, unless so designated by other documentation.

14. ABSTRACT

15. SUBJECT TERMS

16. SECURITY CLASSIFICATION OF:			17. LIMITATION OF ABSTRACT	15. NUMBER OF PAGES	19a. NAME OF RESPONSIBLE PERSON
a. REPORT	b. ABSTRACT	c. THIS PAGE			David Pine
UU	UU	UU	UU		19b. TELEPHONE NUMBER 212-998-7744

RPPR Final Report
as of 11-Jan-2022

Agency Code: 21XD

Proposal Number: 70394MS **Agreement Number: W911NF-17-1-0328**
INVESTIGATOR(S):

Name: David J. Pine
Email: pine@nyu.edu
Phone Number: 2129987744
Principal: Y

Organization: **New York University**
Address: 665 Broadway, New York, NY 100122331
Country: USA
DUNS Number: 041968306 EIN: 135562308
Report Date: 19-Oct-2021 Date Received: 17-Nov-2021
Final Report for Period Beginning 20-Jul-2017 and Ending 19-Jul-2021
Title: Self-Assembly of Colloidal Diamond and Related Lattices for 3-D Photonic Band Gap Materials
Begin Performance Period: 20-Jul-2017 **End Performance Period:** 19-Jul-2021
Report Term: 0-Other
Submitted By: David Pine Email: pine@nyu.edu
Phone: (212) 998-7744

STEM Degrees: **STEM Participants:**

Major Goals: The major overarching goal of this project was to develop a method using colloidal self-assembly to fabricate photonic crystals that exhibit a full omnidirectional 3D photonic band gap (PBG) at optical and near-infrared frequencies.

As originally conceived and proposed, we planned to do this by self-assembling a colloidal superlattice isomorphic to the metallic compound MgCu2, which is one of several so-called Laves phases and consists of two sublattices, one cubic diamond, and the other pyrochlore. The idea was to self-assemble this structure and then selectively remove the (sacrificial) pyrochlore sublattice leaving only the diamond sublattice, which would be used as a template for making an inverse diamond photonic crystal. However, as we made progress toward this goal, we developed a new method by which we could directly self-assemble a cubic diamond lattice from colloidal particles without the need for a sacrificial sublattice. The new method eliminated the need to remove the pyrochlore sublattice, which made it simpler and more robust than the original method. Thus, while the overall goal of the project did not change, the means by which we planned to achieve our goals shifted to this new more direct self-assembly route.

Last year (2020), we published a demonstration of our new method to directly self-assemble a stand-alone colloidal crystal with a cubic diamond crystal structure. This appeared in the journal Nature in October 2020. The self-assembly of colloidal diamond had not been done previously. This represented a major breakthrough as the diamond lattice is generally considered to be the best crystalline lattice for making a material with a full photonic band gap (PBG).

The diamond lattice as assembled from the polymer colloidal particles we employ does not have a photonic band gap as the dielectric contrast between the particles and the matrix (water or air) is not large enough to open up a band gap. Instead, the self-assembled diamond lattice serves as a template for an inverse diamond lattice, that is, a lattice in which the interstices of the colloidal diamond lattice are filled with a high-refractive-index, optically non-absorbing, material and the colloidal template is removed so that only air remains where there were once colloidal particles. While both the direct lattice (one made up of high-index particles) and the inverse lattice (one where the interstices are filled with a high-index material), have a photonic band gap, the band gap is generally wider for the inverse lattice, making an inverse lattice is more desirable.

The key goals and activities related to our colloidal self-assembly project were:

1. Self-assemble colloidal crystals with a cubic diamond structure. Then increase the size of the diamond crystals

so they are at least 50 microns across, with an ultimate target of 1 mm or larger.

2. Understand the phase behavior of assemblies of tetrahedral clusters so that we can optimize the formation of cubic diamond crystals. This includes understanding the nucleation and growth of the crystals so we can optimize their growth and limit defect formation. There are a number of parameters we can vary to optimize the self-assembly of colloidal diamond crystals. One set of parameters pertains to the geometry of our patchy colloidal tetramers that serve as the building block. These include the compression ratio, which governs the interlocking mechanism that fixes the requisite eclipsed conformation, and the size ratio, which governs how the patches on the different particles interact.

3. We use complementary DNA "sticky ends" tethered from patches within the clusters. The placement of these patches and their functionalization with DNA provides a critical ingredient for directing the self-assembly of the clusters. Understanding, controlling, and optimizing this interaction is important for optimizing the growth of diamond crystals and for controlling the formation of defects. However, having succeeded in making diamond crystals using DNA-coated patches on our colloidal tetrahedra, we believe it may be possible to use attractive patch-patch interactions other than DNA to direct the self-assembly, in particular the depletion, hydrophobic, or electrostatic interactions.

4. Optimizing and characterizing photonic band gaps. We need to optimize the photonic band structure by varying the geometry of the clusters so that the diamond colloidal crystals formed exhibit the widest possible band gaps. Our introduction of compressed tetrahedral clusters as the building block of a diamond structure introduces a new geometry whose optical properties need to be assessed (in contrast to the well-studied diamond lattice made from spheres). In addition, in order to measure the photonic band structure completely, we need to grow our new diamond crystals in different orientations, that is, with different crystalline planes parallel to the substrate. To accomplish this, we need to develop surface templates that can seed the growth of the diamond crystals along different crystalline planes.

5. The diamond crystals we make from polymer-based colloids serve as templates for the photonic crystals with full PBGs. After assembling the colloidal diamond crystals, we need to back-fill them with a high dielectric material, TiO2 for band gaps in the visible and TiO2 or Si for band gaps in the infrared, to make inverse photonic crystals from our colloidal diamond templates. One goal is to perfect the sol-gel process for back-filling the colloidal template with TiO2, as both the inverse diamond and inverse pyrochlore lattices exhibit superior band gaps to their direct lattice counterparts. A related goal is to perfect the atomic layer deposition (ALD) of TiO2 and chemical vapor deposition of Si.

6. A final goal is to characterize the optical properties of the structures we make, including their photonic band structure and the optical consequences of disorder and defects. In many ways, this is where the most interesting physics lies. Controlling defects will allow us to suppress spontaneous emission, which is interesting from a fundamental viewpoint and also important for making improved optical devices. Exploring disorder may lead to Anderson localization of light, a long-sought but elusive goal in the propagation of classical waves.

Accomplishments: See uploaded attachment

RPPR Final Report
as of 11-Jan-2022

Training Opportunities: Over the course of the grant, training was provided for three graduate students (Mr. Johnathon Gales, Mr. Mingxin He, and Ms. Jeana (Aojie) Zheng) and three postdocs (Dr. Étienne Ducrot, Dr. Mingxin He, and Dr. Fan Cui).

Mr. Mingxin He successfully defended his Ph.D. in May 2020 and then rejoined the research effort as a postdoc in June 2020, continuing through February 2021. He moved to Cornell where he works as a postdoctoral associate in the group of Nicholas Abbott in the Chemical and Biomolecular Engineering Department. His principal activities were particle synthesis, characterization, and self-assembly. He worked closely with Mr. Gales.

Mr. Johnathon Gales was supported for three years under this grant during his Ph.D. studies in the Physics Department at NYU. His principal activities were computer simulation of self-assembly, calculation, design, and optimization of optical properties of photonic crystals, templating and growth of colloidal crystals, inversion of photonic crystals to make band gaps in the near IR, and characterization. He is expected to finish his Ph.D. in 2022.

Ms. Jeana (Aojie) Zheng received half of her support from this grant for one year. She investigated the diffusion of DNA-bound particles, which is relevant to the annealing and growth of DNA-coated colloidal crystals. She is expected to finish her Ph.D. in 2022.

Dr. Étienne Ducrot was supported for one year under this grant. He performed computer simulations for the self-assembly of the MgCu2 colloidal crystal superstructure and of the diamond lattice. These studies were used to understand the self-assembly process and to optimize the design of the particles so that they would self-assemble into the desired structures. He also helped direct the laboratory work of Mr. He and Mr. Gales.

Dr. Fan Cui has supported for 7 months at 65.5% under this grant. She helped synthesize particles and she performed experiments with a total internal reflection microscope she build to measure the interaction potentials and binding between DNA-coated particles, which was important for understanding and tuning the interactions between our DNA-coated colloids.

The research activities of these students and postdocs over the course of this grant are summarized in the section Accomplished Under Goals. They received training on various experimental techniques, including light scattering, video particle tracking, particle synthesis, cleanroom activities, numerical simulations, optical and electron microscopy, and a number of other techniques.

In addition to the direct research training they received, they all participated in weekly group meetings with me and the rest of my research group where they presented and discussed their research progress. These meetings are open discussions and provide a supportive and lively forum for them to engage in scientific discussions.

All four participated in the weekly meetings of the Center for Soft Matter Research in the Physics Department at NYU. Each one of them had to give two formal 20-minute talks, with 10 more minutes for discussion and questions, over the course of the year. After the lockdown of the labs in March 2020, these meetings continued remotely using Zoom software.

As detailed in the section on Dissemination, all of the students and postdocs presented the results of their research at various national meetings, in particular at the annual March Meeting of the American Physical Society. During the COVID-19 pandemic, this participation occurred remotely over the internet; otherwise, oral presentations were made in person.

RPPR Final Report
as of 11-Jan-2022

Results Dissemination: Papers published supported by this grant

1. Patchy Colloidal Clusters with Broken Symmetry
You-Jin Kim, Jae-Hyun Kim, In-Seong Jo, David J. Pine, Stefano Sacanna, and Gi-Ra Yi
J. Am. Chem. Soc. 2021, vol 143, 13175Ð13183
Publication Date: August 15, 2021
https://doi.org/10.1021/jacs.1c05123

2. Colloidal Particles with Triangular Patches
Mingxin He, Johnathon P. Gales, Xinhang Shen, Min Jae Kim, and David J. Pine
Langmuir 2021, vol 37, 7246Ð7253
Publication Date: June 3, 2021
https://doi.org/10.1021/acs.langmuir.1c00877

3. Colloidal diamond
Mingxin He, Johnathon P. Gales, ƒtienne Ducrot, Zhe Gong, Gi-Ra Yi, Stefano Sacanna & David J. Pine
Nature 2020, vol 585, 524Ð529
https://doi.org/10.1038/s41586-020-2718-6

This paper was listed by Web of Science as both a "Highly Cited Paper" (top 1% of the academic field of Physics based on a highly cited threshold for the field and publication year) and as a "Hot Cited Paper" (top 0.1% of papers in the academic field of Physics.)

4. DNA functionalization of colloidal particles via physisorption of azide-functionalized diblock copolymers
Jeongbin Moon, In-Seong Jo, Jeong Hoon Yoon, Yeongha Kim, Joon Suk Oh, David J. Pine and Gi-Ra Yi
Soft Matter 2019, vol 15, 6930Ð6933
https://doi.org/10.1039/c9sm01243e

5. DNA-Coated Microspheres and Their Colloidal Superstructures
Jeongbin Moon, In-Seong Jo, Etienne Ducrot, Joon Suk Oh, David J. Pine & Gi-Ra Yi
Macromolecular Research 2018 vol 26, 1085Ð1094

6. Pyrochlore lattice, self-assembly and photonic band gap optimizations
ƒtienne Ducrot, Johnathon Gales, Gi-Ra Yi, and David J. Pine
Optics Express 2018, vol 26, 30052-30060

Articles submitted supported by this grant

1. Effect of Photon Counting Shot Noise on TIRM
Fan Cui, Sophie Marbach, Jeana Aojie Zheng, Miranda Holmes-Cerfon, David J. Pine
arXiv 2111.06468 (2021)

2. Comprehensive view of microscopic interactions between DNA-coated colloids
Fan Cui, David J. Pine
arXiv 2111.06468 (2021)

Over the course of the grant period, I (the PI) gave invited talks about this work at the following venues. Please note that several conferences that the PI was scheduled to speak at were canceled because of the COVID-19 pandemic (ACS National Meeting in Philadelphia, Imagine Nano Conference in Bilboa, Spain).

1. Workshop on Nanofabrication by Self-Assembly, NYU, 2017 October 13.

2. Symposium at the University of Pennsylvania in honor of Prof. Tom Lubensky 2017 November 4.

3. Self-Assembly of Colloidal Systems 2018 Bordeaux, France 2018 September 20.

4. Anisotropic Particles Meeting Konstanz, Germany 2018 September 27.

5. CNRS Research Workshop (GDR 3535) Bordeaux, France 2018 October 23.

6. CCNY Salzberg Chemistry Seminar New York, NY 2018 December 10.

7. Colloidal Science and Metamaterials Meeting Paris, France 2019 February 27.

8. APS March Meeting Short Course Boston, MA 2019 March 3.

9. UMass Chemical Engineering Colloquium Amherst, MA 2019 April 2.

10. UCSB Chemical Engineering Colloquium Santa Barbara, CA 2019 April 11.

11. Kent State Liquid Crystals Institute Kent, OH 2019 April 17.

12. Soft Materials Gordon Research Conference New London, NH 2019 August 11.

13. 12th Northeast Complex Fluids & Soft Matter Workshop, Manhattan College, Bronx 2020 January 20.

14. Wayne State University Department of Physics & Astronomy Colloquium, 2020 January 20.

15. Future Materials, Materials Science & Nanotechnology Conference, Lisbon, Portugal, 2020 February 26.

16. Department of Chemical Engineering Colloquium, City Colege of New York, CUNY, 2020 March 9.

17. Nonlinear Physics/Statistical Physics/Complex Systems/Soft Matter Seminar (Remote) Technion, Tel Aviv, Weizmann Bar-Ilan, Ben Gurion, Hebrew University, 2020 August 25.

18. Center for Nanoscale Materials Colloquium (Remote), Argonne National Laboratories, 2020 September 16.

19. Workshop on Molecular and Colloidal Self-Assembly (Remote), Korean Academy of Science and Technology (KAST) 2020 November 23.

20. Department of Physics Colloquium (Remote), Hunter College, 2020 December 9.

21. Department of Chemical, Biological, & Materials Engineering Colloquium, University of South Florida, 2021 February 10.

22. Raman Research Institute Colloquium (Remote), Bangalore, India, 2021 March 11.

23. March Meeting of the APS Invited Talk (Remote), 2021 March 19.

Papers published supported by this grant

1. Patchy Colloidal Clusters with Broken Symmetry
You-Jin Kim, Jae-Hyun Kim, In-Seong Jo, David J. Pine, Stefano Sacanna, and Gi-Ra Yi
J. Am. Chem. Soc. 2021, vol 143, 13175Ð13183
Publication Date: August 15, 2021
https://doi.org/10.1021/jacs.1c05123

2. Colloidal Particles with Triangular Patches
Mingxin He, Johnathon P. Gales, Xinhang Shen, Min Jae Kim, and David J. Pine
Langmuir 2021, vol 37, 7246Ð7253
Publication Date: June 3, 2021
https://doi.org/10.1021/acs.langmuir.1c00877

3. Colloidal diamond
Mingxin He, Johnathon P. Gales, ƒtienne Ducrot, Zhe Gong, Gi-Ra Yi, Stefano Sacanna & David J. Pine
Nature 2020, vol 585, 524Ð529

https://doi.org/10.1038/s41586-020-2718-6

4. DNA functionalization of colloidal particles via physisorption of azide-functionalized diblock copolymers
Jeongbin Moon, In-Seong Jo, Jeong Hoon Yoon, Yeongha Kim, Joon Suk Oh, David J. Pine, and Gi-Ra Yi
Soft Matter 2019, vol 15, 6930Ð6933
https://doi.org/10.1039/c9sm01243e

5. DNA-Coated Microspheres and Their Colloidal Superstructures
Jeongbin Moon, In-Seong Jo, Etienne Ducrot, Joon Suk Oh, David J. Pine & Gi-Ra Yi
Macromolecular Research 2018 vol 26, 1085Ð1094

6. Pyrochlore lattice, self-assembly, and photonic band gap optimizations
ƒtienne Ducrot, Johnathon Gales, Gi-Ra Yi, and David J. Pine
Optics Express 2018, vol 26, 30052-30060

The postdoc working on the grant, Dr. ƒtienne Ducrot, and the graduate students, Ms. Aojie Zheng and Mr. Johnathon Gales, gave contributed talks at the 2019, 2020, & 2021 March Meeting of the American Physical Society in Boston, MA.

Several conferences that the PI was scheduled to speak at were canceled because of the COVID-19 pandemic (ACS National Meeting in Philadelphia, Imagine Nano Conference in Bilboa, Spain). Nevertheless, there were a few opportunities to speak over the reporting period of the past year. I (the PI) gave invited talks about this work at the following venues:

Honors and Awards: The PI, David Pine, was elected to the American Academy of Arts and Sciences. See https://www.amacad.org/content/members/newfellows.aspx?s=a

Protocol Activity Status:

Technology Transfer: Nothing to Report

PARTICIPANTS:

Participant Type: PD/PI
Participant: David Pine
Person Months Worked: 3.00 **Funding Support:**
Project Contribution:
National Academy Member: N

Participant Type: Co PD/PI
Participant: Stefano Sacanna
Person Months Worked: 3.00 **Funding Support:**
Project Contribution:
National Academy Member: N

Participant Type: Graduate Student (research assistant)
Participant: Johnathon Gales
Person Months Worked: 15.00 **Funding Support:**
Project Contribution:
National Academy Member: N

Participant Type: Graduate Student (research assistant)

RPPR Final Report
as of 11-Jan-2022

Participant: Jeana (Aojie) Zheng
Person Months Worked: 6.00 **Funding Support:**
Project Contribution:
National Academy Member: N

Participant Type: Postdoctoral (scholar, fellow or other postdoctoral position)
Participant: Fan Cui
Person Months Worked: 5.00 **Funding Support:**
Project Contribution:
National Academy Member: N

Participant Type: Postdoctoral (scholar, fellow or other postdoctoral position)
Participant: Mingxin He
Person Months Worked: 2.00 **Funding Support:**
Project Contribution:
National Academy Member: N

Participant Type: Postdoctoral (scholar, fellow or other postdoctoral position)
Participant: Etienne Ducrot
Person Months Worked: 15.00 **Funding Support:**
Project Contribution:
National Academy Member: N

Participant Type: Staff Scientist (doctoral level)
Participant: Andrew Hollingsworth
Person Months Worked: 15.00 **Funding Support:**
Project Contribution:
National Academy Member: N

Participant Type: Faculty
Participant: Gi-Ra Yi
Person Months Worked: 3.00 **Funding Support:**
Project Contribution:
National Academy Member: N

ARTICLES:

RPPR Final Report
as of 11-Jan-2022

Publication Type: Journal Article Peer Reviewed: Y **Publication Status:** 1-Published
Journal: Chemical Communications
Publication Identifier Type: DOI Publication Identifier: 10.1039/C8CC03637C
Volume: 54 Issue: 60 First Page #: 8328
Date Submitted: 8/31/19 12:00AM Date Published:
Publication Location: Cambridge, England, UK
Article Title: Compressible colloidal clusters from Pickering emulsions and their DNA functionalization
Authors: In-Seong Jo, Joon Suk Oh, Shin-Hyun Kim, David J. Pine, Gi-Ra Yi
Keywords: microspheres; crystallization; nanoparticles; spheres
Abstract: Colloidal clusters were prepared by assembling azide-functionalized non-crosslinked polymer particles using fluorinated oil-in-water emulsion droplets. The particles were adsorbed onto the droplet interface, which were packed to form clusters during slow evaporation of the oil. Then, the clusters were coated by DNA using an alkyne–azide cycloaddition (SPAAC) reaction. As the particles are not crosslinked, the shape of the DNA-coated clusters can be further modified to control the compression ratio through plasticization.
Distribution Statement: 3-Distribution authorized to U.S. Government Agencies and their contractors
Acknowledged Federal Support: **Y**

Publication Type: Journal Article Peer Reviewed: Y **Publication Status:** 1-Published
Journal: Optics Express
Publication Identifier Type: DOI Publication Identifier: 10.1364/OE.26.030052
Volume: 26 Issue: 23 First Page #: 30052
Date Submitted: 8/31/19 12:00AM Date Published: 10/1/18 12:00AM
Publication Location:
Article Title: Pyrochlore lattice, self-assembly and photonic band gap optimizations
Authors: Étienne Ducrot, Johnathon Gales, Gi-Ra Yi, David J. Pine
Keywords: MOLECULAR-DYNAMICS SIMULATIONS; CLUSTERS; CRYSTALS
Abstract: Non-spherical colloidal building blocks introduce new design principles for self-assembly, making it possible to realize optical structures that could not be assembled previously. With this added complexity, the phase space expands enormously so that computer simulation becomes a valuable tool to design and assemble structures with useful optical properties. We recently demonstrated that tetrahedral clusters and spheres, interacting through a DNA-mediated short-range attractive interaction, self-assemble into a superlattice of interpenetrating diamond and pyrochlore sublattices, but only if the clusters consist of partially overlapping spheres. Here we show how the domain of crystallization can be extended by implementing a longer range potential and consider how the resultant structures affect the photonic band gaps of the underlying pyrochlore sublattice. We show that with the proper design, using clusters of overlapping spheres lead to larger photonic band gaps that open up at lower
Distribution Statement: 3-Distribution authorized to U.S. Government Agencies and their contractors
Acknowledged Federal Support: **Y**

Partners

,

RPPR Final Report
as of 11-Jan-2022

I certify that the information in the report is complete and accurate:
Signature: David Pine
Signature Date: 11/17/21 4:34PM

Accomplished under Goals

COVID-19 impact

Before presenting what was accomplished under this grant, I note that because of the COVID-19 pandemic, our research labs were completely closed down from early March 2020 through the end of June 2020. Even when we were allowed access to my research group's labs in late June 2020, many of the shared facilities that we use were not available. Among these were NYU's scanning electron microscope (SEM), which is needed to evaluate our colloidal particles, NYU's atomic layer deposition (ALD) apparatus, needed to make the inverse diamond crystals required to make samples with a photonic band gap, and the facilities at the Advanced Science Research Center (ASRC) at the City University of New York (CUNY) in Harlem. The SEM became available in early August 2020. The ALD has only been available since about July 2021 and while it does work, it was damaged due to lack of proper maintenance during the COVID-19 crisis, and as a results works at somewhat reduced capacity.

Goal 1

The major accomplishment under this grant was the development of the first, and as of this writing, the only method to self-assemble a cubic colloidal diamond lattice suitable making materials with a full omnidirectional 3D photonic band gap.[1]

The method starts with the development of a method to synthesize a new kind of colloidal particle: a particle with four patches nestled between four spherical lobes arranged with tetrahedral symmetry, as illustrated in Fig. 1. The method for making the particle, shown in Fig. 1(a) involves assembling four micrometer-size charged polymer colloids (shown in white) around an oppositely-charged polymerizable oil droplet. The polymer colloids are lightly plasticized so that they partially coalesce, which extrudes out the central oil droplet so that it forms four patches (light blue). The oil droplet is then polymerized to form four solid patches (red) and functionalized with single-stranded DNA with sticky ends. A scanning electron microscope image of particles made this way is shown in Fig. 1(b).

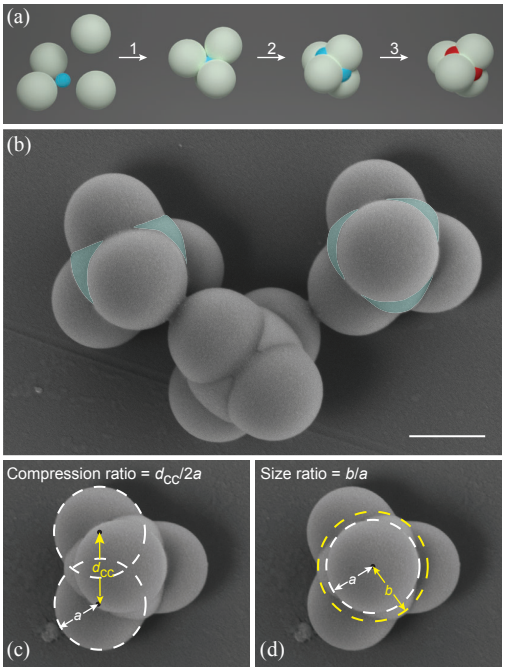

Figure 1: Four-patch, four-lobe colloidal particles. (a) Synthesis. (b) Scanning electron microscope image. The patches of two particles are artificially colored blue. (c) Geometrical parameters: compression ratio and size ratio.

The second step is the self-assembly of these particles into a cubic diamond lattice. In a cubic diamond lattice of spheres, each sphere is four-fold coordinated with its neighbors, as illustrated in Fig. 2(a). This represents a major challenge for self-assembly as simple spheres need at least six contacts for mechanical stability. Moreover, the spheres occupy a very small fraction of the available volume, achieving a maximum volume fraction of 34% for spheres that touch (not illustrated). These numbers should compared to face-centered cubic, which self-

assemblies readily, in which each particle has twelve nearest neighbors and the maximum packing fraction for touching spheres is 74%; for body-centered cubic, there are eight nearest neighbors with a maximum packing fraction of 68%. To coax colloidal particle to have only four nearest neighbors, we synthesize colloidal particles with four tetrahedrally arranged sticky patches, where binding is provided by self-complementary single-stranded DNA. However, this is not enough to produce a cubic diamond lattice since it does not control the local conformations of spheres. In principle, spheres can be arranged locally so that they are either in the *eclipsed* or *staggered* conformation, as illustrated in Fig. 2(b). All particles in a cubic diamond crystal are always arranged in the staggered conformation.

Figure 2(c) illustrates how our new particle design solves each of these problems. First, in contrast to spherical patchy particles, the patches on the four-lobe particles can only bind to each other if the particles adopt an eclipsed conformation. Second, the four-lobe particles fill a much greater fraction of the available volume, typically around 65%, and are much more highly constrained than the spherical patchy particles, which are free to adopt any local conformation. This renders the packing much more stable for self-assembly. Figures 2(d) and (e) show the unit cell of a cubic diamond crystal made from such particles.

As noted above, the (colored) patches of our four-lobe particles are selectively functionalized with single-stranded DNA, which makes the patches mutually attractive while the rest of the four-lobe particle remains very nearly hard-sphere repulsive. Our ability to selectively functionalize the patches with DNA relies on subtle chemistry we have developed that keeps the polymerizable oil from dissolving into the PS particles. Because the DNA-mediated attraction is temperature dependent, we can control the self-assembly of these particles by maintaining the system at or just below the DNA melting temperature, typically around 40°C, which allows fairly large crystals to grow.

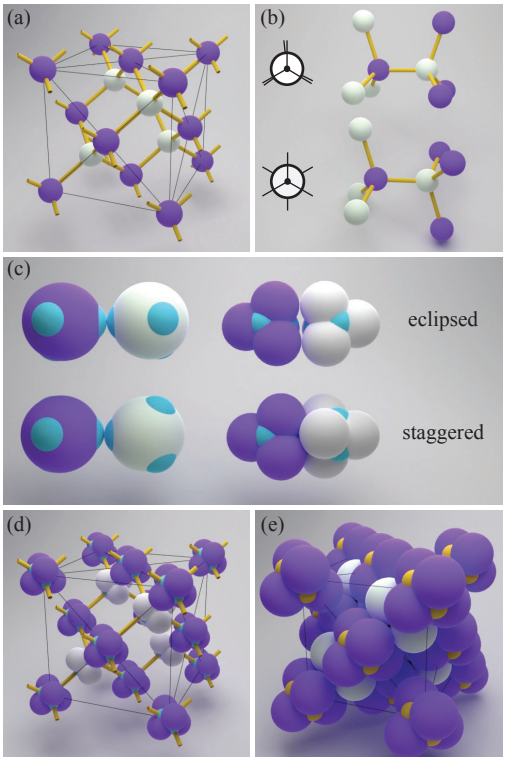

Figure 2: Self-assembly of colloidal cubic diamond. (a) Diamond crystal of (small) spheres. (b) Eclipsed (top) and staggered (bottom) conformation of tetrahedrally-coordinated particles. (c) Binding of spherical particles with patches (left). Binding of four-lobe particles with patches (right). (d) Diamond lattice of artificially small four-lobe particles with patches to show bonding coordination and conformation. (e) Diamond lattice of four-lobe particles with patches in correct proportions so that lobes correctly interlock.

Figure 3 shows two photographs of the 111 plane of self-assembled diamond crystals, one taken with a fluorescent optical microscope and the other with an SEM. The tetrahedral patches, actually extend into the core of each particle in between the four lobes. This core contains a green fluorescent dye, which can be imaged using a fluorescent optical microscope. When a diamond crystal is formed, the fluorescent cores produce a hexagonal honeycomb pattern, like those shown in Fig. 3(a). The diamond crystalline grains extend over tens of micrometers, with a typical size of 40 to 50 μm. Confocal microscopy reveals that the crystals extend at least tens of micrometers into the sample confirming that the crystals are are fully three-dimensional cubic diamond.

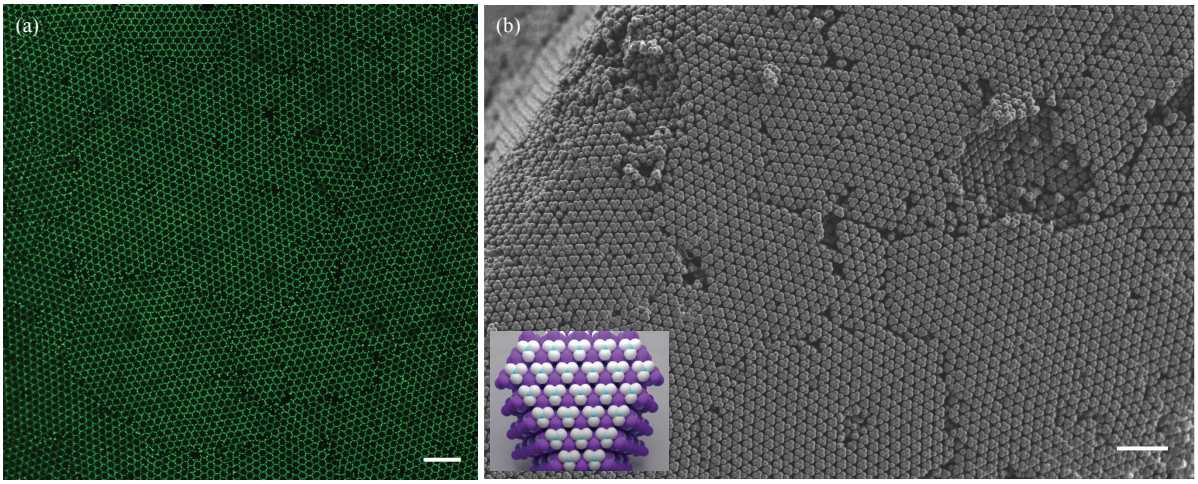

Figure 3: (a) Fluorescent optical microscope image of a cubic diamond colloidal crystal self-assembled from our four-patch, four-lobe particles. The hexagonal honeycomb pattern is from the [111] face of a diamond crystal. (b) Scanning electron microscope (SEM) image of a dried diamond crystal. The inset shows a model of the expected structure for a diamond lattice, which corresponds closely to the SEM image. Scale bars are 5 μm.

The diamond crystals we make are sufficiently dense and constrained that they can be dried without destroying the crystal structure. This is essential for subsequent processing in which the crystal is inverted with a high-refractive index material. In Fig. 3(b), we show an electron microscope image of one such dried crystal. These crystals serve as templates for the inverted photonic crystals, which is discussed under Goal 6.

In order to grow larger single diamond crystals, we started developing surface patterns on substrates that can serve as templates to seed the growth of single diamond crystals that are at least a millimeter across. While the effort is still in its infancy, it is already showing great promise. In Fig. 4(a), we show a simple surface pattern consisting of a triangular array of raised triangles with a circular hole in the center. One of the triangular bases of a four-lobe particle sits in the triangular depression to form the first layer of the [111] plane of a colloidal diamond lattice, while the circle at the center of the raised triangle serves as a template for the second layer, which is inverted relative to the first so that one lobe of a four-lobe particle sits in the circle. Figure 4(b) shows a the first two layers of a diamond crystal growing in perfect registry with the surface template. Indeed, the crystalline bilayer remains in registry over the full 1 millimeter of the surface template, suggesting that single crystals at least 1 mm in size can be successfully grown using surface templates.

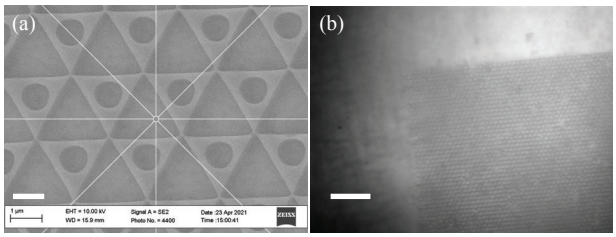

Figure 4: Surface-templating of colloidal diamond crystals. (a) SEM image of surface template made using electron-beam lithography. Scale bar = 1 μm. (b) Bilayer of colloidal diamond self-assembled on surface-patterned template. Scale bar = 10 μm.

The surface templates are formed on silicon wafers using electron-beam lithography with spin-coated PMMA as a resist. The exposed areas of PMMA are selectively washed away using standard solvents, leaving the unexposed PMMA layer with the patterned holes, revealing the silicon substrate below.

Finally, we note that during the first phase of this project, we were pursuing a different means for self-assembling a diamond lattice, which involved self-assembling a colloidal superlattice isomorphic to the metallic compound $MgCu_2$, which is one of several so-called Laves phases and consists of two sublattices, one cubic diamond, and the other pyrochlore, as shown in Fig. 5.[2] The idea was to self-assemble this lattice and then to remove the pyrochlore lattice, leaving behind the diamond lattice. To this end, we performed Brownian dynamics simulations of the self-assembly process using the HOOMD-blue simulation package to help determine the optimal conditions for self-assembling the $MgCu_2$ structure.[3–5] While there is nothing indicating that this method cannot work, it is much more more complicated than our new method so we decided to abandon this approach in favor of the new method that directly forms a diamond lattice.

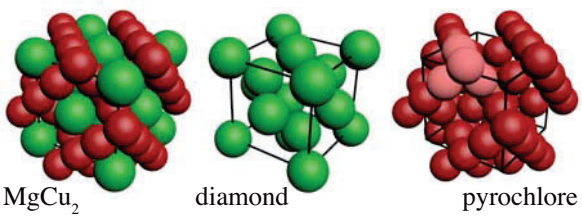

Figure 5: $MgCu_2$ structure with interpenetrating diamond (green) and pyrochlore (red) sublattices. Maximum packing is achieved with ratio of the radii of green (R) and red (a) particles is $R/a = \sqrt{3/2} \simeq 1.225$. The pale red color in pyrochlore structure shows one of the tetrahedral clusters that make up the pyrochlore lattice.

Goal 2

To better understand and optimize the self-assembly of diamond crystals from our four-lobe patchy particles, we performed Brownian dynamics simulations of the self-assembly process using the HOOMD-blue simulation package.[4,5] The shape of the four-lobe patchy particles is critical to self-assembling diamond crystals. We characterize the shape by two parameters, the compression ratio and the size ratio, which are defined in Fig. 1(c) and (d).

At the same time, we synthesized four-lobe patchy particles with a wide range of compression and size ratios to compare with the simulations. The results of our experiments, shown in the phase diagram in Fig. 6, are largely consistent with our simulations, although the range of parameters over which diamond crystals form is somewhat smaller than is indicated in experiments. Of the two parameters, the compression ratio is the more important for the optical properties. Fortuitously, as we will see below, the range of compression ratios over which diamond crystals form corresponds to those for which the photonic band gap is widest in the inverse diamond crystals we aim to make.

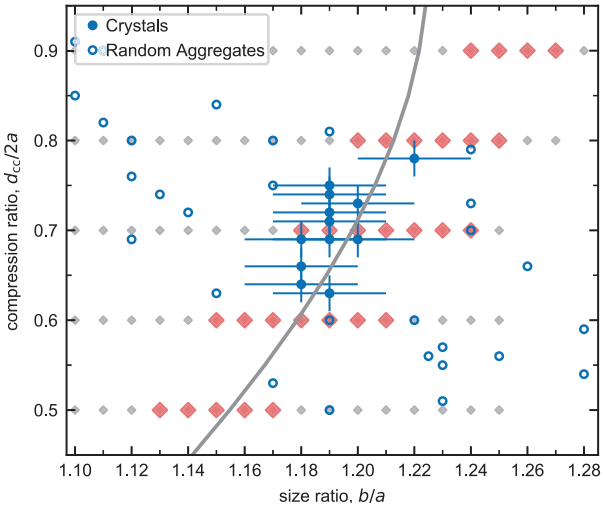

Figure 6: Phase diagram showing range of compression and size ratios over which diamond crystals form. The blue circles show the results of our experiments: solid circles indicate where diamond crystals formed; open circles indicate where amorphous structures formed. The diamonds show the results of our simulations: red diamonds indicate where diamond crystals formed; gray diamonds indicate where amorphous structures formed.

We explored some other physical conditions under which the diamond crystals form. For the particles we used, we found that it was necessary to suspend them in a mixture of normal and heavy water, roughly in a one-to-one ratio, so that the tetrahedral patchy clusters we nearly density

matched to the water. We leave a small density difference between the particles and the solvent (water) so that the gravitational height is about 20 μm, which supports a particle concentration gradient that facilitates crystal formation. This works very well and leads to large single crystals, typically on the order of 50 to 120 μm across. To grow larger crystals, we plan to continue and expand upon the surface templating scheme described in the previous section.

In another study, we developed spherical particles with tetrahedrally coordinated *triangular* patches.[6] Here, the idea was to explore the use of the shape of *patches* rather than the shape of the particles to enforce a particular conformation. The method of synthesis was similar to that of the four-lobe patchy particles but in this case the four lobe are allowed to completely coalesce when plasticized, as shown in Fig. 7. The idea was that the the eclipsed conformation would be enforced by the triangular patches,[7] which would align to attain the highest degree of patch overlap. Eclipsed conformations, in contrast to the staggered conformations needed to assemble colloidal diamond, should lead to colloidal clathrates. Unfortunately, the patches we were able to synthesize were too small and had too great of a curvature to enforce any particular conformation. In the end, the particles self-assembled into either chains or random structures with low coordination numbers (2–4). We also demonstrated a number of other structures, including some made from three-lobe particles with triangular patches,[6] illustrating the versatility of the colloidal fusion approach we employed.[1,8]

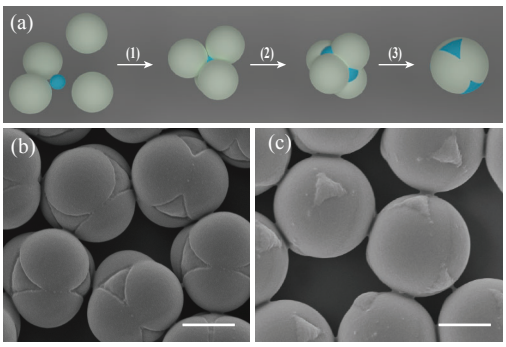

Figure 7: Patchy particles with four triangle patches. (a) Controlled deformation of the colloidal clusters with polymerization of the patches before the deformation is complete, allowing the patches to maintain a triangular shape. (b) SEM micrograph of partially compressed colloidal tetramers after polymerizing the liquid oil droplet. (c) SEM micrograph of tetra-patch particles with eclipsed triangular patches.

In the first phase of this grant, we also explored the effect of the range of the interparticle attractive potential on the self-assembly of the $MgCu_2$ superlattice with Brownian dynamics simulations using the HOOMD-blue package.[3–5] Perhaps the most important result of these simulation was that it showed that using a softer attractive potential between the spheres and clusters greatly expands the range of compression and size ratios over which the $MgCu_2$ structure forms.

Goal 3

The use of DNA-coated patches to create an attractive interaction between patches works well. One very convenient feature of the interaction is it is easily and conveniently controlled by varying the temperature by a few degrees. We can localize the DNA on the patches to a sufficiently high degree particles always bind to each other in the proper *eclipsed* conformation required for the cubic diamond crystal structure we seek. Thus, in some sense, *Goal 3* has largely been accomplished.

There are some disadvantages of using DNA, however. First, it is expensive, which would be a concern if we needed to make diamond crystals in large quantities. Second, the binding kinetics are slow, which makes crystal growth times somewhat long. Therefore, to address these concerns, we have started experiments to explore using interactions other than DNA hybridization, including the depletion interaction and electrostatic interactions between oppositely charged patches. This work, while very promising, is still in the early stages and will be an active area of research for us in the next phase of research.

Goal 4

The diamond crystals we make are unconventional in that they are made from compressed tetrahedral clusters rather than spheres (see Fig. 1). Moreover, there are a number of variable design parameters that are expected to affect the photonic properties of the crystals, including whether the lattice is direct or inverted, the dielectric contrast, the dielectric filling fraction, and the compression ratio of the particles (see Fig. 1(c)). To understand and optimize the photonic properties, we calculated the photonic band structure for diamond crystals made from our tetrahedral clusters for various design choices using the MIT Photonic Bands software.[9]

Figure 8(a) shows the photonic band diagram for an inverse diamond lattice of compressed clusters with a compression ratio $r_{cc}/2a = 0.74$, which is readily achievable experimentally. A rendition of the structure is shown in Fig. 8(c). This structure produces a PBG between the 2nd and 3rd bands, just as for other crystals with diamond symmetry. In this case, we used the refractive index of silicon, 3.45 in the near IR where optical communication networks typically operate (1.5 μm). Here, the band gap has a relative width of $\delta \equiv \Delta f/f_c = 0.14$, where f_c is the center frequency of the band gap, which in this case is about $1.73fa/c$, where f is the frequency of the

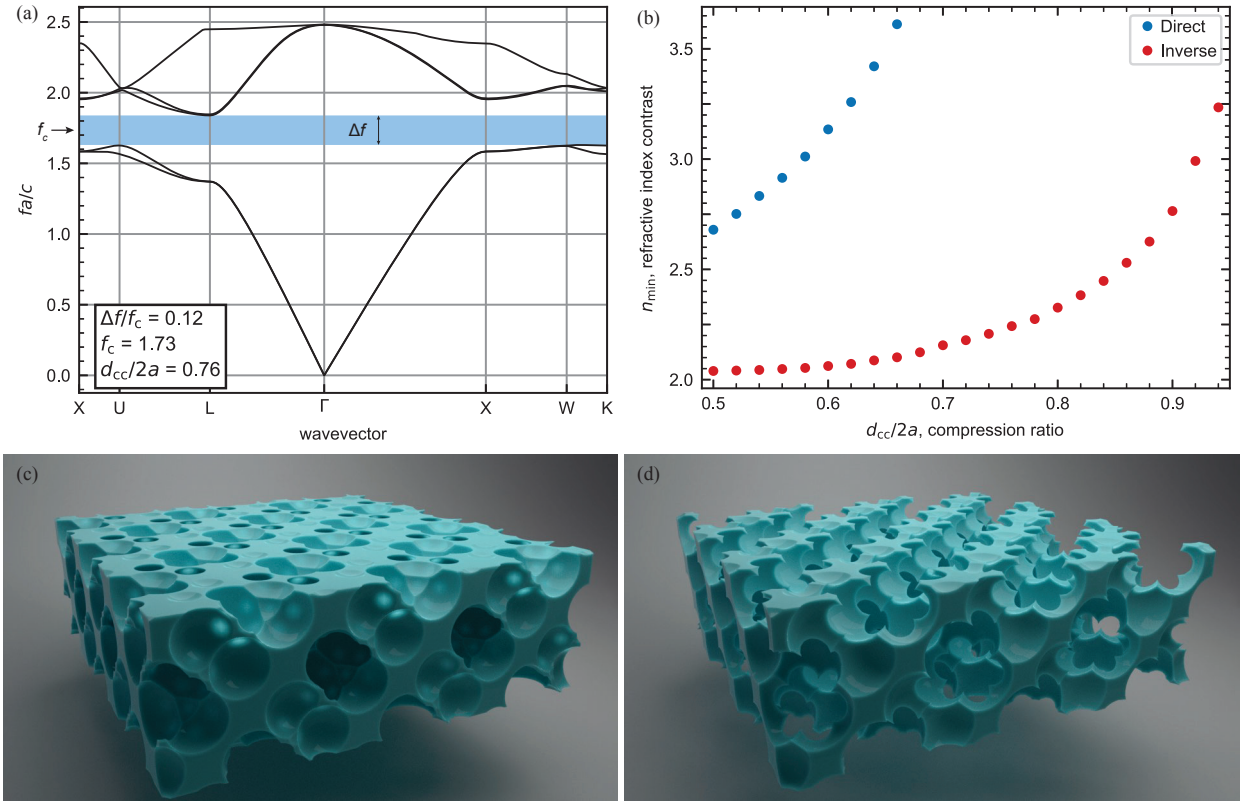

Figure 8: Photonic properties and structure of inverse cubic diamond lattice of clusters. (a) Band diagram for an inverse diamond lattice of clusters with a compression ratio of 0.76 (the structure shown in (c) below), showing a complete photonic band gap with relative width 0.12 between the second and third bands (highlighted in blue). Only the first five bands are shown but the first 50 were calculated: no other band gaps were found. (b) Minimum index at which a band gap opens for a range of compression ratios: direct lattice, blue; inverse lattice, red. (c) Structure for a compression ratio of 0.76. The size ratio is chosen so that patches just touch. The volume fraction of solid material is 0.32. (d) Same structure as in (c), but made using a sacrificial layer with a thickness of 10% of the radius of the spherical lobe of a cluster. The volume fraction of solid material is 0.20.

light, a is the lattice constant, and c is the speed of light in vacuum.

Figure 8(b) shows the minimum refractive index contrast for which a band gap opens up for the direct and inverse lattices as a function of the particle compression ratio. The figure shows that in all cases, a band gap opens up at lower refractive index contrast for the inverse lattice than for the direct lattice.

Figure 9 shows how the relative width of the band gap changes as the compression ratio is varied from 0 (a diamond lattice of nonoverlapping spheres) to 1 (a diamond lattice of uncompressed clusters) for refractive indices of 2.6 (titania) and 3.4 (silicon). These calculations reveal that using compressed clusters ($0.1 \lesssim d_{cc}/2a \lesssim 0.8$) opens up a band gap for the inverse lattice where there was none for nonoverlapping spheres ($d_{cc}/2a = 0$). The widest band gap is achieved a little below or above a compression ratio of 0.6, depending on the value of the refractive index. Fortuitously, this is very near the compression ratios that we have already found to crystallize experimentally: $0.63 \leq d_{cc}/2a \leq 0.78$, indicated by light blue in Fig. 9. By contrast, using compressed clusters only slightly improves the band gap for the direct lattice, with the widest band gap occurring near $d_{cc}/2a = 0.15$ and diminishing to 0 when $d_{cc}/2a = 0.6$. In all of these calculations, the size ratio is fixed so that the patches touch precisely when the spherical lobes touch for neighboring particles in the staggered conformation. Variations in the size ratio have very little effect on the band gap.

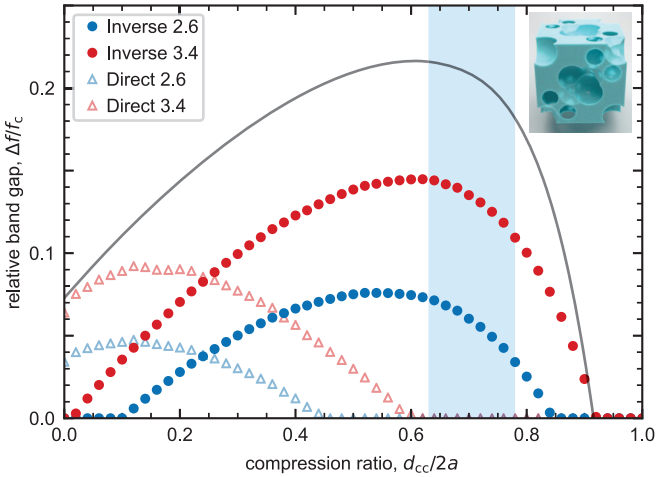

Figure 9: Relative band gap vs. compression ratio. Circles and triangles correspond to direct and inverse lattices, respectively. Blue and red points correspond to titania ($n = 2.6$) and silicon ($n = 3.4$), respectively. The experimental values for the compression ratio found to crystallize in experiments are highlighted in light blue, showing that the maximum band gap widths for the inverse cluster cubic diamond are realized near the experimental conditions. The gray lines shows the band gap obtained for an inverse silicon lattice where a sacrificial layer of thickness $0.1a$ is used to coat the colloidal template before backfilling with silicon. Inset: Inverse cubic diamond unit cell with compression ratio of particles in the direct lattice $d_{cc}/2a = 0.76$.

Goal 5

As discussed above, an inverse diamond lattice exhibits a wider band gap than a direct lattice and is thus more desirable. Moreover, as the polymer particles used to self-assemble a direct diamond lattice have a refractive index of only 1.59, which is well below the value needed to open up a band gap (see Fig. 8), this direct lattice does not provide a viable means to realize a materials with a photonic band gap. Therefore, we use the direct diamond lattice of polymer particles as a template for making an inverse structure in which the interstices are filled with a high-dielectric material and the polymer particle template is removed leaving behind only air (see Fig. 8).

To make inverse diamond photonic crystals with a band gap in the near IR, which is highly desirable for optical communications, we use silicon which has a refractive index of about 3.45; for a band gap in the visible, we use TiO_2, which has a refractive index of 2.4–2.8 (depending on processing details), the highest of any optically nonabsorbing material in the visible. We employ

different methods to make these inverse lattices: low-pressure chemical vapor deposition (CVD) for silicon and sol-gel chemistry for TiO_2.

We discuss our results for making an inverse silicon lattice first, which uses CVD to deposit silicon in the template interstices. We cannot directly perform CVD on the polymer crystal template because the method requires heating the sample to 550°C, which would melt the polymer before the silicon could be deposited. Therefore, we use ALD, which can be done at about 70°C, well below the softening temperature of polystyrene (105°C), to deposit a thin protective layer of alumina, typically about 50 nm, although thicker protective layers can be used. Following ALD, CVD is used to fill the interstices with silicon, which also removes the polymer template leaving behind a porous silicon network. We typicallly overfill the interstices, meaning that the sample exterior is coated with a solid thin later of silicon. This thin solid layer can be removed using a focused ion beam (FIB) to reveal the porous structure below, as shown in Fig. 10(a). Using FIB to cut vertically through the sample shows that the silicon completely backfills the pores or the polymer template all the way down to the silicon wafer substrate some 15 μm below, as shown in Fig. 10(b).

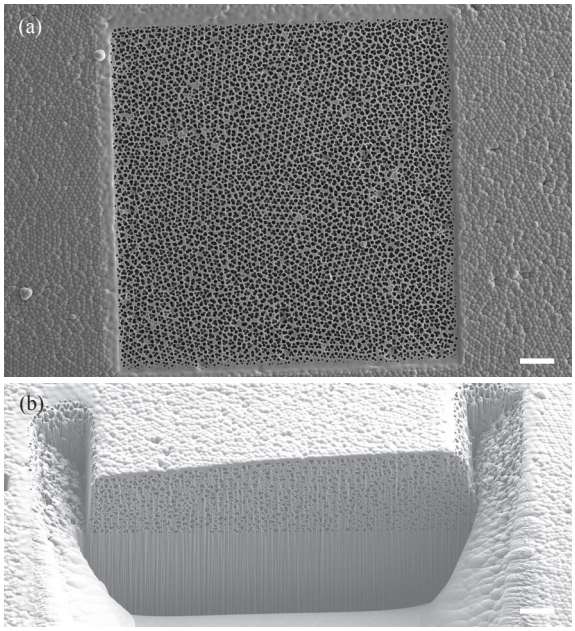

Figure 10: SEM images of inverse silicon structure made using CVD. (a) The solid silicon overlayer has been removed over at 100 μm × 100 μm area using a focused ion beam to reveal the templated porous silicon photonic crystal below. (b) Cutting into the sample vertically with a focused ion beam shows that the sample is porous all the way down to the silicon wafer substrate. Scale bars = 10 μm.

While not shown here, the thin alumina protective layer can be etched chemically to leave only porous silicon. Our calculations show that the effect of removing the alumina layer is to *widen* the band gap. For example, in Fig. 9, we show that removing such a layer increases the width of the band gap by more than 50%.

These initial results are very promising. However, the diamond crystal structure is degraded during extraction of the polymer template from the capillary tubes in which the colloidal crystals are grown. This is the source of the disorder visible in the images in Fig. 10. We believe this can be remedied by growing the colloidal crystals directly on the silicon (or other material) substrate, a strategy we are currently pursuing.

Next we discuss our results for making inverse titania (TiO_2) lattices using sol-gel chemistry. Here we start from the polymer colloidal templates used to make the inverse silicon structures. In this method, the colloidal template is dried and then backfilled with a solution of titanium isopropoxide, the TiO_2 precursor. The solution is allowed to dry and then is backfilled again. After repeating this process several times, the solution is gelled at room temperature and then the sample heated to 500°C. Gelation preserves the inverse structure while heating (calcining) burns out the polymer template and organic part of the titania precursor. The result is initially amorphous titania which is subsequently converted to the crystalline anatase form at high temperatures, as confirmed by x-ray diffraction. A refractive index of 2.6 is measured for anatase using ellipsometry. Figure 11(a) shows an inverse face-centered-cubic (FCC) photonic crystal made in this way; Fig. 11(b) shows a disordered inverse diamond structure. The disordered diamond suffers from the same

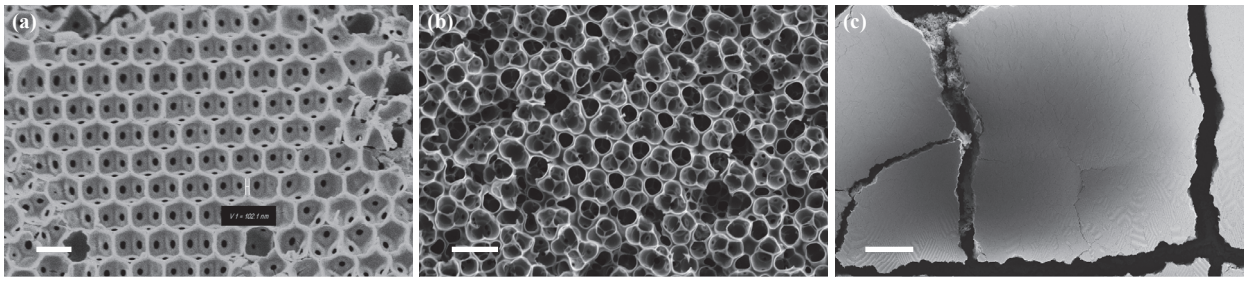

Figure 11: Inverse TiO_2 photonic crystals. (a) Inverse FCC photonic crystal. Scale bar = 1 μm. (b) Inverse disordered diamond structure. Scale bar = 2 μm. (c) Inverse FCC photonic crystal. Scale bar = 100 μm.

problem discussed above of having its structure degraded during extraction of the polymer template from the capillary tubes in which the colloidal crystals are grown. Again, we are addressing this problem by developing a process that grows the crystals directly on a substrate outside of a capillary tube.

Samples undergo considerable shrinkage during calcination, which inevitably leads to cracking. Thus, a major challenge for this method is the control of shrinkage and, much more importantly, cracking. Initially, our samples exhibited cracks on length scales ranging from 5 to 40 μm. However, we found we could greatly reduce the cracking by using ALD to first lay down a 50-nm titania coating on our polymer template, which is then followed by the sol-gel approach. We also found that controlling the heating rate during calcination also reduced cracking, with about 3°C/min being optimal. Figure 11(c) shows an inverse FCC porous titania structure made using sol-gel templating. Here the distance between cracks is quite large, typically several hundred micrometers, which is quite acceptable. Using ALD puts down a TiO_2 layer that is much denser than that created by the sol-gel process and thus reduces shrinkage and cracking. Backfilling the entire structure with ALD, however is very expensive and time consuming. By contrast, backfilling using a sol-gel process is very inexpensive and relatively fast. Our approach of using ALD to put down a thin coating followed by backfilling using a sol-gel process takes the best advantage of both approaches for efficiently making large inverse titania photonic crystals.

Goal 6

The optical characterization of our materials will be undertaken as soon as the inverse photonic crystals are available. The most straightforward measurements to make are optical reflection and transmission measurements, which can be compared to finite-difference time-domain (FDTD) calculations, which we detailed above.

The principal method for characterizing the optical properties of photonic crystals is transmittance and reflectance spectroscopy. For measurements in the near-IR, this is best done using an FTIR spectrometer microscope, as this allows one to measure the photonic properties of small crystallites, say 20 μm to several millimeters across (lateral dimensions), as well as the spatial variations in the optical properties that might occur due to localized defects.

The most definitive and convincing characterization of a photonic band gap is to measure the fluorescent lifetime of a dye, contained in the photonic crystal, that emits in the band gap. As stated previously, we are aiming to build a material with photonic band gap at 1.5 μm, which is where optical communication networks typically operate. We are working with a group at the University of Vienna who has synthesized a suitable fluorophore for this purpose.

References

1. He, M., Gales, J. P., Ducrot, É., Gong, Z., Yi, G.-R., Sacanna, S. & Pine, D. J. Colloidal diamond. *Nature* **585,** 524–529 (2020).
2. Ducrot, É., He, M., Yi, G.-R. & Pine, D. J. Colloidal alloys with preassembled clusters and spheres. *Nat. Mater.* **16,** 652–657 (2017).
3. Ducrot, É., Gales, J., Yi, G.-R. & Pine, D. J. Pyrochlore lattice, self-assembly and photonic band gap optimizations. *Opt. Express* **26,** 30052 (2018).
4. HOOMD-blue. *https://codeblue.umich.edu/hoomd-blue/* (2010).
5. Glaser, J., Nguyen, T. D., Anderson, J. A., Lui, P., Spiga, F., Millan, J. A., Morse, D. C. & Glotzer, S. C. Strong scaling of general-purpose molecular dynamics simulations on GPUs. *Comput. Phys. Commun.* **192,** 97–107 (2015).
6. He, M., Gales, J. P., Shen, X., Kim, M. J. & Pine, D. J. Colloidal Particles with Triangular Patches. *Langmuir* **37,** 7246–7253 (2021).
7. Romano, F. & Sciortino, F. Patterning symmetry in the rational design of colloidal crystals. *Nat. Commun.* **3,** 975 (2012).
8. Gong, Z., Hueckel, T., Yi, G.-R. & Sacanna, S. Patchy particles made by colloidal fusion. *Nature* **550,** 234–238 (2017).
9. Johnson, S. G. & Joannopoulos, J. D. Block-iterative frequency-domain methods for Maxwell's equations in a planewave basis. *Opt. Express* **8,** 173–190 (2001).